

## **A HARMONIC-SUPPRESSED MICROSTRIP ANTENNA USING A METAMATERIAL-INSPIRED COMPACT SHUNT-CAPACITOR LOADED FEEDLINE**

**Omar F. Siddiqui<sup>1, 2, \*</sup> and Ashraf S. Mohra<sup>3</sup>**

<sup>1</sup>Department of Electrical and Computer Engineering, University of Waterloo, Ontario, Canada

<sup>2</sup>College of Engineering, Taibah University, Madinah, Saudi Arabia

<sup>3</sup>Electronics Research Institute, Cairo, Egypt

**Abstract**—This paper presents a novel method to suppress the higher order harmonics in the microstrip patch antennas. A practical 0.75 GHz microstrip patch antenna is fed with a quarter-wave feedline designed by exploiting the dispersion properties of shunt-capacitor-loaded transmission-line metamaterials. It is shown that two higher order harmonic modes at 1.25 and 1.5 GHz are completely eliminated. In addition, there is about a one-fourth reduction in the length of the impedance matching quarter-wave feedline.

### **1. INTRODUCTION**

Although theoretically investigated in 1967 by Veselago [1], it was not until 2001 that the concept of negative refraction was experimentally demonstrated in the synthesized periodic structures that consist of highly resonant split rings and thin metallic wires [2]. Since then, there has been a phenomenal growth in the metamaterial research activities worldwide. For example, see the books [3, 4] and the review paper by Ramakrishna [5] and the references therein. The term ‘metamaterial’ was initially applied specifically to the negative-index materials. But later with the application of negative refraction in other technologies, the scope of the term ‘metamaterial’ has been expanded to also represent other artificial structures such as loaded transmission-line (TL) media [6] and photonic crystals [7]. The TL-metamaterials are based on the equivalent circuit of the split-ring

---

*Received 5 July 2013, Accepted 5 November 2013, Scheduled 15 November 2013*

\* Corresponding author: Omar Farooq Siddiqui (ofsiddiqui@yahoo.com).

and thin-wire metamaterial [8]. Therefore, when extended to two- or three-dimension configurations, TL-metamaterials also demonstrate sub-diffraction focusing properties [9, 10]. Simpler 1D configuration referred to as metamaterial transmission lines (MMTLs) have been employed to build compact devices such as phase-shifters, power dividers, filters, and antennas [11–15]. Band-pass filters have also been designed by using shunt-capacitor loaded lines (shunt-C MMTLs) which employ an extra capacitor loading to control the band-pass response [16, 17].

In all these applications, higher order dispersion characteristics are either not studied or have actually been utilized to design dual-band microwave devices. In many wireless communication applications, the suppression of the higher order harmonics (spurious radiation) is required as they create unwanted interference with other devices. Particularly, the unwanted higher-order radiations from antennas need to be controlled because of the high power ‘spill-over’ into the harmonic bands. Due to their unique dispersion properties, the MMTLs if properly designed have the ability to effectively suppress unwanted bands. Particularly, the dispersion of shunt-C MMTLs can be tailored to achieve bandpass response in the desired frequency range and band-reject response in the undesired spectrum.

This paper proposes a compact shunt-C metamaterial feed-line for a 0.75 GHz microstrip patch that can suppress two harmonic modes that radiate at 1.25 and 1.5 GHz. The metamaterial feed, in this case, serves dual purpose of being a harmonic suppresser and a quarter-wave transformer. Moreover, the size of the feed-line is reduced to about one-fourth of its size when printed using the conventional approach. Similar harmonic suppression techniques include the application of complimentary split ring resonators underneath the microstrip transmission line feed [18]. However, it requires long feed-lines to physically accommodate the resonators. On the other hand, the present technique employs chip components; thereby, the feed length is drastically reduced.

## 2. THE DESIGN APPROACH

Traditionally, the MMTLs have been fabricated by loading a host transmission line with series capacitance and shunt inductance, as depicted in Fig. 1(a). The devices based on this approach exploit the dispersion properties of the fundamental backward-wave mode and the second order forward-wave mode. The MMTL is thus operated under

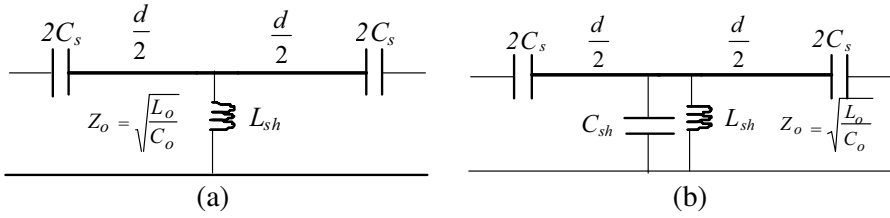


**Figure 1.** Unit cell of metamaterial transmission-line (a) the traditional approach and (b) with an added shunt capacitive loading.

the balanced impedance condition, i.e.,

$$Z_o = \sqrt{\frac{L_o}{C_o}} = \sqrt{\frac{L_{sh}}{C_s}} \quad (1)$$

where  $Z_o$  is the intrinsic impedance of the host transmission line. If the phase velocity of the host medium is assumed to be ‘ $u$ ’ then the distributed inductance and capacitance can be given by  $L_o = Z_o/u$ ,  $C_o = 1/Z_o u$ . Under condition (1), the fundamental and second order bands are connected without the presence of the band-gap. In the current application, a band-gap is needed between the first two bands of the periodic structure. Hence the Fig. 1(a) unit cell is further loaded with a shunt capacitor, as depicted in Fig. 1(b). Although, this can also be achieved by disturbing the impedance balance given by (1), the advantage of adding the shunt capacitance will be obvious later in this section.

Assuming the shunt-C MMTL extends to infinity, the following dispersion relation is obtained by using the Bloch-Floquet theorem [19]:

$$\cosh kd = \cos \beta d \left[ 1 + \frac{YZ}{4} \right] + \frac{j}{2} \sin \beta d [ZY_o + YZ_o] + \frac{YZ}{4} \quad (2)$$

$kd$  is the Bloch propagation constant,  $\beta = \omega\sqrt{L_o C_o}$  is the intrinsic phase constant of the unloaded line,  $\omega$  is the radian frequency, and  $Y$  and  $Z$  are the series admittance and shunt impedance of the loading elements, given by:

$$Y = \frac{1}{j\omega L_{sh}} + j\omega C_{sh}, \quad Z = \frac{1}{j\omega C_s} \quad (3)$$

For the conventional MMTL,  $C_{sh} = 0$  and  $Y = 1/j\omega L_{sh}$ . A simplified version of Equation (2), which gives more insight into the resonance behavior of the structure can be obtained by assuming the intrinsic and Bloch phase shift ( $\theta_B \approx Kd$ ) per unit cell to be much less than

unity ( $\beta d$  and  $kd \ll 1$ ) [8]:

$$\theta_B = \omega \sqrt{L'C'} \left[ \left( \frac{1}{\omega^2 L' C_s} - 1 \right) \left( \frac{1}{\omega^2 L_{sh} C'} - 1 \right) \right] \quad (4)$$

where

$$L' = L_o d \quad \text{and} \quad C' = C_o d + C_{sh} \quad (5)$$

The periodic structure has two resonances which are represented by the two bracketed terms in the above equation. These resonances mark the cut-off frequencies of the shunt-C MMTL. To further illustrate the operation, a representative dispersion curve is plotted in Fig. 2. The band-gap is given by  $(f_H - f_L)$  and is controlled by the series and shunt inductances and capacitances. Comparing the plots of the exact phase shift (solid line) and the approximate phase shift (dotted line), it can be observed that they are in good agreement for smaller shifts (less than  $0.5\pi$  as mentioned in the derivation of (4)). In terms of the two band-edge frequencies  $f_H$  and  $f_L$ , the phase relation can be written as:

$$\theta_B = \omega \sqrt{L'C'} \left[ \left( \frac{\omega_H^2}{\omega^2} - 1 \right) \left( \frac{\omega_L^2}{\omega^2} - 1 \right) \right] \quad (6)$$

where

$$\omega_H = \frac{1}{L' C_s} \quad \text{and} \quad \omega_L = \frac{1}{L_{sh} C'} \quad (7)$$

Note that, as depicted in Fig. 2, the dispersion region for which ( $kd < bd$ ) is called the light cone where leaky radiation modes exist. The solution of the unknown parameters requires the Bloch impedance equation which can be obtained under similar phase constraints [17]:

$$Z_B^2 = \frac{L' \omega_H^2 - \omega^2}{C' \omega_L^2 - \omega^2} \quad (8)$$

Observing (7) and (8), the advantage of the shunt loading capacitance  $C_{sh}$  can be demonstrated. In the absence of  $C_{sh}$ , the determination of  $L'$  and  $C'$  establishes the intrinsic impedance and, consequently, the width of the microstrip host medium. If the designer selects the width, then one of the cut-off frequencies cannot be pre-specified leaving an uncontrollable bandwidth. Furthermore, as inferred from (5) the inclusion of  $C_{sh}$  reduces the periodicity  $d$  of the host medium resulting in more compact feed lines.

For known values of the design frequency  $\omega = \omega_{des}$  Bloch phase shift,  $\theta_B$  Bloch impedance  $Z_B$ , and the cut-off frequencies  $f_H$  and  $f_L$ , Equations (6) and (8) can be solved to determine the  $L'$  and  $C'$ :

$$C' = \frac{\omega_{des} \theta_B}{Z_B (\omega_L^2 - \omega_{des}^2)}, \quad L' = \frac{\omega_{des} Z_B \theta_B}{\omega_H^2 - \omega_{des}^2} \quad (9)$$

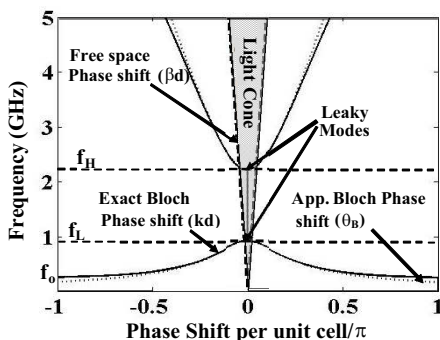


**Figure 2.** Brillouin diagram of the MM line using the current design of the MM feed.

The series capacitor and the shunt inductor can then be determined by using (7) and (9):

$$C_s = \frac{\omega_H^2 - \omega_{des}^2}{\omega_{des}\omega_H^2 Z_B \theta_B}, \quad L_{sh} = \frac{Z_B(\omega_L^2 - \omega_{des}^2)}{\omega_{des}\omega_L^2 \theta_B} \quad (10)$$

The periodicity and the shunt capacitance are obtained by using the following relation:

$$d = \frac{L'}{L_o} \quad \text{and} \quad C_{sh} = C' - C_o d \quad (11)$$

Finally, the Bragg’s frequency  $f_o$  which signifies the start of the backward-band is given by:

$$f_o = \frac{1}{4\pi\sqrt{L_{sh}C_s}} \quad (12)$$

### 3. THE HARMONIC SUPPRESSION PATCH

To demonstrate the harmonic suppressing, a microstrip patch antenna is designed that radiates at 0.75 GHz. If a Rogers 5880 substrate with a dielectric constant 2.2 and a thickness 31 mils is used, the dimensions of the patch are given by 134 mm × 158 mm and its input impedance is given by 225 ohms. Hence, a quarter-wave line of length 75 mm having a characteristic impedance of 100 ohm is used to feed the patch for the baseline simulations and measurements. The simulations are performed by Zeland’s IE3D simulator and the return loss measurements are done using the Anritsu 37369C vector network analyzer. The results are depicted in Fig. 3. In addition to the

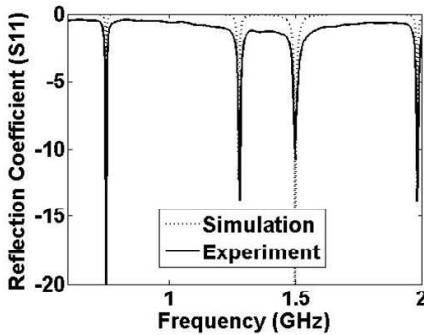


**Figure 3.** A comparison of simulation and measurement for the regular quarter wave feedline microstrip patch antenna.

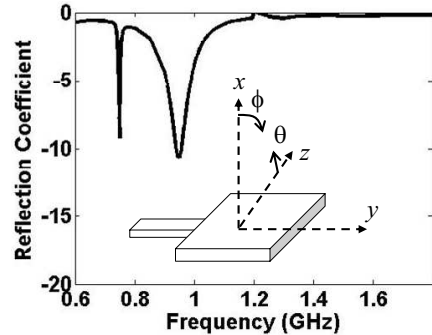


**Figure 4.** The simulated reflection coefficient for the microstrip patch fed by a metamaterial transmission line. The inset shows the patch schematics to identify the  $E$ -plane and  $H$ -plane of the patch antenna.

fundamental frequency of 0.75 GHz, spurious radiation modes can be seen at approximately 1.25 and 1.5 GHz.

To suppress the higher order harmonics, the quarter-wave metamaterial feed should be designed such that the band-gap ( $f_H - f_L$ ), (Fig. 2) spans the spurious radiation region. The cut-off frequencies are assumed to be  $f_L = 0.9$  GHz, and  $f_H = 2.2$  GHz. Assuming a four cell MMTL, the Bloch phase shift (per unit cell) used in the design equation is given by  $\theta_B = \pi/8$  radians. Setting  $\omega_{des} = 0.75$  GHz, and the Bloch impedance ( $Z_B$ ) equal to  $100 \Omega$  in (6)–(11) and rounding the quantities to the nearest commercially available component gives  $L_{sh} = 15$  nH,  $C_s = 4.5$  pF,  $C_{sh} = 2$  pF and  $d = 2$  mm. Note that to accommodate for the Rogers substrate  $u = 2.27 \times 10^8$  m/s is used which is obtained by using the LineCalc<sup>®</sup> package by Agilent. Furthermore, the Bloch impedance is set to  $100 \Omega$  to match the antenna of impedance  $225 \Omega$  to the  $50 \Omega$  microstrip system. The phase velocity is further applied in the calculation of the distributed inductance and capacitance of the microstrip line.

The simulated  $S_{11}$ , depicted in Fig. 4, shows the disappearance of the harmonic patch modes at 1.25 and 1.5 GHz. The  $S_{11}$  dip in the frequency response at 0.75 GHz well corresponds to the design. The simulated  $E$ - and  $H$ -plane radiation patterns at the fundamental frequency (0.75 GHz) are shown in Fig. 5. Not shown here are the patterns of a regular patch which can be seen in any reference such

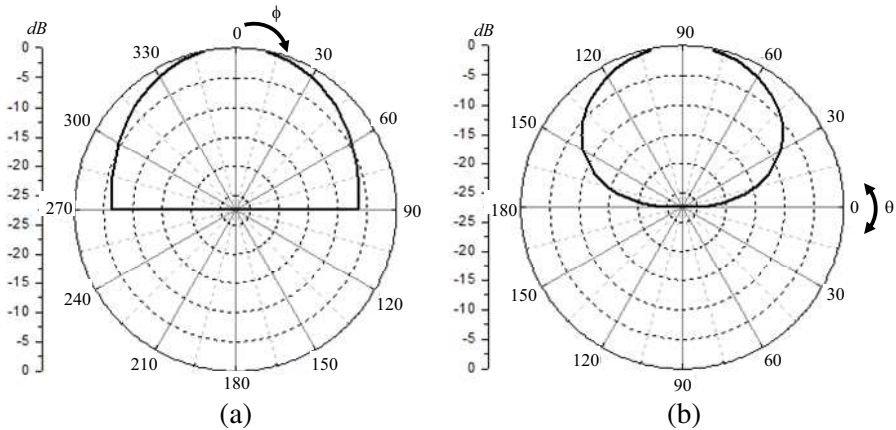


**Figure 5.** The simulated  $E$ - and  $H$ -plane radiation patterns at 0.75 GHz for the MM-fed patch antenna. (a)  $E$ -plane pattern. (b)  $H$ -plane pattern.

as [20]. It can be observed that the MMTL feed does not affect the radiation of the patch. However, a leaky wave mode is observed at 0.95 GHz which arises due to the propagation of electromagnetic waves within the light cone where the free space phase and Bloch phase are related by  $Kd < \beta d$  (see the Brillouin diagram Fig. 2) [21]. The leaky-wave modes are inherent to periodic structures and their locations are mainly dependent on the periodicity ( $d$ ) if the lumped element values are kept constant. Let us look at the leaky wave condition by equating the phase shift per unit cell for the MMTL (4) to the equation of the light line ( $\omega\sqrt{L_0C_0d}$ ) and approximating in the lowest band ( $f < f_L$ ) results in the following equation:

$$\omega^4 = \frac{1}{L_{sh}C_sL_0d\sqrt{C_0d(C_0d + C_{sh})}} \quad (13)$$

Hence, keeping the inductances and capacitances constant, the leaky-wave modes can be shifted to higher frequencies by reducing the periodicity ' $d$ '. To demonstrate this effect in the current design, the value of periodicity is changed from 2 mm to 0.5 mm in simulation. As shown in Fig. 6, this results in a shift of 30 MHz (0.95 to 0.98 GHz) in the leaky-wave mode frequency. More drastic changes in the leaky-wave frequency can be obtained by changing the lumped element values, particularly the shunt capacitance  $C_{sh}$ . Consider reducing the shunt capacitance from 2 pF to 1.75 pF. Consequently, the leaky-wave mode shifts from 0.95 to 1.01 GHz. Further shifts can be obtained by

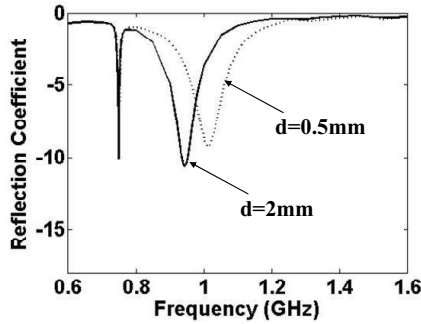


**Figure 6.** Effect of change in the periodicity on the leaky-wave frequency.

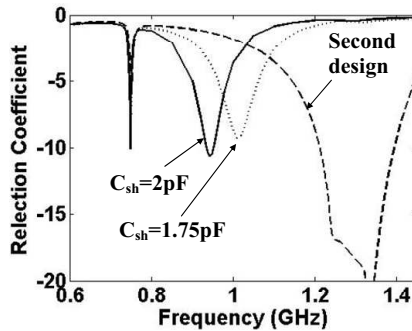


**Figure 7.** Effect of change in the lumped element design on the leaky-wave frequency. The second design refers to the case in which the cut-off frequencies are changed so that the leaky wave mode is shifted to 1.3 GHz.

redesigning the MMTL with a different band-gap. Consider the case when the band gap is redefined from  $f_L = 1.2$  GHz to  $f_H = 2$  GHz. From Equations (6)–(11), the lumped element values are then given by  $L_{sh} = 35$  nH,  $C_s = 4.5$  pF, and  $C_{sh} = 0.3876$  pF. This case is labeled as ‘second design’ in Fig. 7. As depicted, the leaky-mode is shifted to 1.3 GHz.

#### 4. FABRICATION AND MEASUREMENTS

The harmonic suppressed microstrip antenna with compact shunt capacitor loaded metamaterial feedline was fabricated and the lumped parameters were soldered. The photograph of the fabricated microstrip

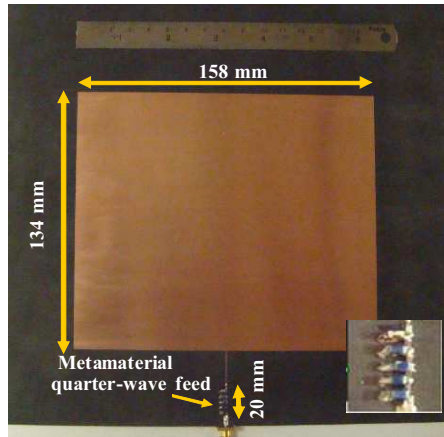


**Figure 8.** Photograph of the realized harmonic suppressed microstrip antenna.

antenna is depicted in Fig. 8. As shown, the quarter-wave shunt-C MMTL segment only acquires 20 mm length in the feed line.

The inset shows the zoomed-in view of the shunt-C MMTL feed.

The return loss measurement and simulation results are shown in Fig. 9. As depicted, the spurious modes at 1.25 and 1.5 GHz are well-suppressed. The antenna is matched at the designed frequency of 0.75 MHz. The simulation and experimental  $S_{11}$  are in good agreement for the fundamental microstrip mode (0.75 GHz). However, the leaky wave dip is shifted to 0.935 GHz in experiment, compared to 0.95 GHz in simulation. This shift in the leaky-wave mode is primarily attributed to the chip component tolerances which are not accounted for in the simulations. It may be noted that the location of leaky modes depends on the choice of the cut-off frequencies, the unit cell length ( $d$ ) and the number of unit cells employed in building the quarter-wave line. Hence, the location of these modes in the spectrum is controllable unlike the higher order harmonics whose locations are inherently governed by the resonant frequency of the patch. Therefore, by proper design strategy (as discussed in previous section), the leaky-wave modes can be placed in the ranges where frequency suppression is not needed or may be utilized in some other application. For bandwidth comparison, the measured reflection coefficients ( $S_{11}$ ) for the MMTL-fed and quarterwave-fed patches are superimposed and are depicted in the inset of Fig. 9. Both of the patches have a (VSWR < 2) bandwidth of about 0.67% which is typical for highly-resonant rectangular patch antennas [22].

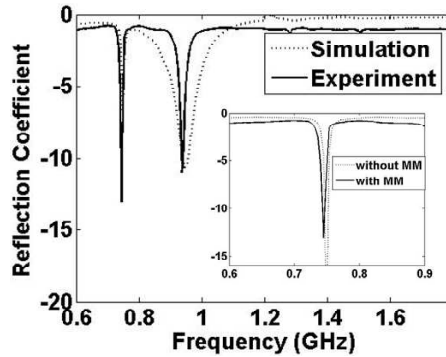


**Figure 9.** A comparison of simulation and measurement for the MMTL-fed harmonic-suppressed microstrip patch antenna. The inset shows a comparison of experimental results for the two patches (with and without MMTL feed) for the frequencies around the resonance.

## 5. CONCLUSIONS

A practical 0.75 GHz microstrip patch antenna with suppressed higher harmonics is presented. The harmonic suppression is accomplished using the shunt-C metamaterial matching feed-line. These types of metamaterial lines have earlier been used in reconfigurable band-pass filters. The harmonic suppressed antenna measurements when compared with the conventional patch show that the spurious modes at 1.25 and 1.5 GHz have been suppressed completely. A leaky radiation mode arises at 1 GHz as a result of the inherent metamaterial. With proper design, the leaky mode can be placed at a desired location where interference suppression is not required or it can be utilized in other applications. It may be noted that the choice of the patch antenna frequency is arbitrary and in this study 0.75 GHz is chosen due to the readily available chip components at the time of the design.

## REFERENCES

1. Veselego, V. G., "The electrodynamics of substances with simultaneously negative values of  $\epsilon$  and  $\mu$ ," *Soviet Physics Uspekhi*, Vol. 10, No. 4, 509–514, Jan.–Feb. 1968.
2. Shelby, R. A., D. R. Smith, and S. Schultz, "Experimental verification of a negative index of refraction," *Science*, Vol. 292, 77–79, Apr. 2001.

3. Eleftheriades, G. V. and K. G. Balmain, *Negative Refraction Metamaterials: Fundamental Principles and Applications*, 1st Edition, John Wiley and Sons, Toronto, 2005.
4. Caloz, C. and T. Itoh, *Electromagnetic Metamaterials: Transmission Line Theory and Microwave Applications*, John Wiley & sons, Inc., 2006.
5. Ramakrishna, S. A., "Physics of negative refractive index materials," *Reports on Progress in Physics*, Vol. 68, No. 2, Feb. 2005.
6. Iyer, A. K. and G. V. Eleftheriades, "Negative refractive index metamaterials supporting 2-D waves," *IEEE MTT-S International Microwave Symposium Digest*, Vol. 2, 1067–1070, Seattle, WA, Jun. 2–7, 2002.
7. Luo, C., S. Johnson, J. D. Joannopoulos, and J. B. Pendry, "All-angle negative refraction without negative effective index," *Physical Review B*, Vol. 65, No. 13, 2011041–2011044, May 2002.
8. Eleftheriades, G. V., O. Siddiqui, and A. K. Iyer, "Transmission line models for negative refractive index media and associated implementations without excess resonators." *IEEE Microwave and Wireless Components Letters*, Vol. 13, No. 2, 51–53, Feb. 2003.
9. Grbic, A. and G. V. Eleftheriades, "Overcoming the diffraction limit with a planar left-handed transmission-line lens," *Phys. Rev. Lett.*, Vol. 92, No. 11, 117403, Mar. 19, 2004.
10. Iyer, A. K. and G. V. Eleftheriades, "Mechanisms of sub-diffraction free-space imaging using a transmission-line metamaterial superlens: An experimental verification," *Applied Physics Letters*, Vol. 92, 131105, Mar. 2008.
11. Eleftheriades, G. V., "Enabling RF/microwave devices using negative-refractive-index transmission-line metamaterials," *Radio Science URSI Bulletin*, No. 312, 57–69, Mar. 2005.
12. Antoniadis, M. A. and G. V. Eleftheriades, "Compact, linear, lead/lag metamaterial phase shifters for broadband applications," *IEEE Antennas and Wireless Propagation Letters*, Vol. 2, No. 7, 103–106, Jul. 2003.
13. Caloz, C., A. Sanada, and T. Itoh, "A novel composite right-/left-handed coupled-line directional coupler with arbitrary coupling level and broad bandwidth" *IEEE Transactions on Microwave Theory and Techniques*, Vol. 52, No. 3, 980–992, Mar. 2004.
14. Antoniadis, M. and G. V. Eleftheriades, "A broadband Wilkinson balun using microstrip metamaterial lines," *IEEE Antennas and Wireless Propagation Letters*, Vol. 4, 209–212, 2005.

15. Sungjoon, L., C. Caloz, and T. Itoh, "Metamaterial-based electronically controlled transmission-line structure as a novel leaky-wave antenna with tunable radiation angle and beamwidth," *IEEE Transactions on Microwave Theory and Techniques*, Vol. 52, No. 12, 2678–2690, Dec. 2004.
16. Siddiqui, O., A. Mohra, and M. Alkanhal, "Design, analysis, and related applications of shunt varactor loaded reconfigurable metamaterial line," *International Journal of Microwave and Optical Technology*, Vol. 4, No. 5, Sep. 2009.
17. Mohra, A. and O. Siddiqui, "A tunable band pass filter based on capacitor-loaded metamaterial lines," *Electronics Letters*, Vol. 45, No. 9, 470–472, Apr. 2009.
18. Ali, A, and H. Zu, "Microstrip patch antenna incorporating negative permittivity metamaterial for harmonic suppression," *The Second European Conference on Antennas and Propagation (EuCAP 2007)*, 1–3, Edinburgh, 2007.
19. Siddiqui, O., M. Mojahedi, and G. V. Eleftheriades, "Periodically loaded transmission line with effective negative refractive index and negative group velocity," *IEEE Trans. on Antennas and Propagation*, Vol. 51, No. 10, 2619–2625, Oct. 2003.
20. Balanis, C., *Antenna Theory — Analysis and Design*, 2nd Edition, 746–747, John Wiley & Sons, Toronto, 1997.
21. Grbic, A. and G. Eleftheriades, "Experimental verification of backward-wave radiation from a negative refractive index metamaterial," *Journal of Applied*, Vol. 92, No. 10, 5930–5935, 2002.
22. Pozar, D. M. and D. H. Schaubert, *Microstrip Antennas: The Analysis and Design of Microstrip Antennas and Arrays*, 157–159, IEEE Press, New York, 1995.